$(AGN)^2$

13. Active Galactic Nuclei - Diagnostics and Physics

Week 15
June 10 (Monday), 2024

updated on 06/07 13:50

선광일 (Kwangil Seon)
KASI / UST

13.4 Densities and Temperatures in the Narrow-Line Gas

- The “narrow” emission lines observed in Seyfer 2 and narrow-line radio galaxies
  - They are much the same as those observed in H II regions and planetary nebulae, except that in the AGNs the range of ionization is considerably greater.
  - Not only [O II], [O III], [N II], [Ne III] are observed, but also [O I], [N I], [Ne V], [Fe VIII], [Fe X].
  - [S II], which is relatively low stage of ionization (10.4 eV), is generally much stronger in the AGNs.
  - Permitted lines of H I, He I, and He II are moderately strong.
  - These narrow lines are emitted by highly-ionized gas, with roughly “normal” abundances of the elements.
  - The standard nebular diagnostic methods may be used to analyze it.
- NLRG Cyg A
  - is a particularly well-studied example. Table 13.2 shows its measured line intensities.
  - The measured H I Balmer-line relative strengths do not fit the recombination predictions. The observed Balmer decrement is steeper that the calculated recombination decrement, just as it is in H II regions.

- Extinction - Balmer decrement
  - was calculated from the Balmer decrement, to give the best overall fit with the recombination decrement for $T = 10^4$ K, $n_e = 10^4\,\mathrm{cm}^{-3}$.
  - The result is $E(B-V) = 0.69 \pm 0.04$, using the standard reddening law.

    More weight has been given to the Hγ/Hβ and Hδ/Hβ ratios.

    The dust extinction corrected value of Hα/Hβ is 3.08, slightly lager than the recombination value of 2.85.

    This increase is real; it results from a **contribution due to collisional excitation of Hα** (Section 11.5).
  - Cyg A is near the galactic equator in the sky. Therefore, some of $E(B-V)$ is due to duet within our Galaxy. Observations of elliptical galaxies near Cyg A indicate that about half its extinction arises within our Galaxy, and the other half in Cyg A itself.

Observed and calculated relative line fluxes in Cyg A

Ion	λ (Å)	Relative Fluxes Measured	Relative Fluxes Corrected	Crab Nebula	Photoionization Model
Hδ	4101	0.17	0.28	0.31	0.26
Hγ	4340	0.32	0.46	0.61	0.47
Hβ	1.00	1.00	1.00	1.00	1.00
Hα	6563	6.61	3.08	3.28	2.85

Table 13.2

Observed and calculated relative line fluxes in Cyg A

Ion	λ (Å)	Relative Fluxes Measured	Relative Fluxes Corrected	Crab Nebula	Photoionization Model
[Ne V]	3346	0.14	0.38	—	0.12
[Ne V]	3426	0.36	0.95	0.46	0.34
[O II]	3727	2.44	5.00	10.3	0.24
[Ne III]	3869	0.66	1.23	1.56	0.53
[Ne III]	3967	0.22	0.40	0.47	0.16
[S II]	4072	0.14	0.23	0.31	
Hδ	4101	0.17	0.28	0.31	0.26
Hγ	4340	0.32	0.46	0.61	0.47
[O III]	4363	0.16	0.21	0.19	0.19
He I	4471	$\leq$0.07	$\leq$0.09	0.28	0.02
He II	4686	0.25	0.28	0.53	0.18
Hβ	1.00	1.00	1.00	1.00	1.00
[O III]	4959	4.08	3.88	2.81	6.3
[O III]	5007	13.11	12.30	8.43	18.1
[N I]	5199	0.40	0.32	—	—
[Fe XIV]	5303	$\leq$0.10	$\leq$0.08	—	0.01
[Fe VII]	5721	$\leq$0.10	$\leq$0.06	—	0.03
[N II]	5755	0.14	0.09	0.11	—
He I	5876	0.13	0.08	0.79	0.06
[Fe VII]	6087	$\leq$0.07	$\leq$0.04	—	0.04
[O I]	6300	2.10	1.10	1.20	1.24
[O I]	6364	0.69	0.35	0.33	0.41
[Fe X]	6375	0.10	0.05	—	0.07
[N II]	6548	3.94	1.90	1.56	0.29
Hα	6563	6.61	3.08	3.28	2.85
[N II]	6583	13.07	6.15	4.69	0.86
[S II]	6716	3.65	1.66	5.00	
[S II]	6731	3.29	1.51	—	
[Ar III]	7136	0.64	0.25	0.38	—
[O II]	7325	0.35	0.13	0.50	—
[Ar III]	7751	0.13	0.043	—	—

- Using one mean extinction law is an extreme oversimplification.
  - Optical properties
    - The Balmer-line method used to correct the measured line intensities of the spectra of H II regions in other galaxies, starburst galaxy nuclei, and ANGs is the same as the one applied in our Galaxy.
    - The extinction law has been derived from our Galaxy within approximately 1 kpc of the Sun.
    - The properties of the dust would no doubt depend on the physical conditions and past history of the regions.
  - Not Extinction but Attenuation
    - The reddening law was derived from measurements of stars, for which extinction occurs both by absorption and scattering all along the line of sight.
    - However, in AGNs, dust absorbs and scatters light, and scattering not only removes photons from the beam toward the observer, it also add photons to it that were originally going in other directions.
    - In spherically symmetric systems, scattering within the line-emitting region has no effect, only the absorption effect would occur.
  - Clumpiness
    - In nearly all observed nebulae, the gas and dust have clumpy, irregular distributions.
  - Using one extinction law is an extreme oversimplification. The only justification is that at present we do not have sufficient information on the observed strengths of emission lines from AGNs.

- Diagnostic information on the physical conditions in the ionized gas in Cyg A.
  - Temperature
    - [O III] (λ4959 + λ5007)/λ4363 = 77 gives $T = (1.5 \pm 0.1) \times 10^4$ K in the [O III] emitting region in the low-density limit ($n_e < 10^4\,\mathrm{cm}^{-3}$) or lower temperature at higher electron density.
    - [N II] (λ6548 + λ6583)/λ5757 = 89 corresponds to $T = 1.0 \times 10^4$ K in the low-density limit.
  - Density
    - [O III] λ3729/λ3726 is a good electron-density diagnostic in H II regions and PNe. However, this ratio cannot be applied in AGNs because their line widths are comparable to or larger than the separation of the two lines (2.8Å, corresponding to ~ 300 km s^{-1}).
    - [S II] λ6716/λ6731 = 1.10 corresponds to $n_E = 3 \times 10^2\,\mathrm{cm}^{-3}$ at $T = 1.0 \times 10^4$ K, or to $n_e = 4 \times 10^2\,\mathrm{cm}^{-3}$ at $T = 1.5 \times 10^4$ K.
    - [S II] emission arises in a less highly ionized region outside the [O III] emitting zone. Thus, the electron density derived from this ratio is not representative of the entire ionized volume. But, it seems unlikely that $n_e > 10^4\,\mathrm{cm}^{-3}$.
  - Abundances
    - Assumes (1) T = 8,500 K for the [S III], [O I], and [N II] emitting regions, (2) T = 12,000 K for H I, He II, and He II, (3) T = 15,000 K for [O III] and [Ne III], (4) T = 20,000 K for [Ne V] and [Fe VII]

- The derived ionic abundances are shown in Table 13.3.
- With a rough allowance for unobserved stages of ionization, these ionic abundances give the approximate elemental abundances shown in Table 13.4.
- Table 13.4 shows that Cyg A has approximately the same composition as in our Galaxy and other observed galaxies with H II regions or starburst nuceli.
- H is the most abundant element; He is less abundant by a factor of ~ 10; O, Ne, N, and C are the most abundant heavy elements.
- Fe is underabundant, which can be understood as due to depletion onto grains, suggesting the existence of dust within the ionized gas.
- These abundances are useful as a starting point for model calculations based on a more specific physical model.

Table 13.3

Relative ionic composition of Cyg A emission-line region

Ion	Abundance	Ion	Abundance
H^+	10^4	O^0	1.9
He^+	5.7×10^2	O^+	1.7
He^{++}	2.4×10^2	O^{++}	1.5
N^0	0.37	Ne^{++}	0.45
N^+	0.88	Ne^{+4}	0.16
		Fe^{+6}	≤ 0.008

Table 13.4

Approximate elemental abundances in Cyg A emission-line region

Element	Abundance	Element	Abundance
H	10^4	Ne	1
He	10^3	S	0.3
N	1	Fe	≤ 0.1
O	4		

- Similar observational data are available for many other NLRGs and Seyfert 2 galaxies.
- Table 13.5 gives a list of mean values of T and n_e determined from the best fits to [O III], [N II], [O II], [S II], and [O I] line ratios in Seyfert 2 and NLRGs.

[Table 13.5] Mean temperatures, electron densities, and extinctions in Seyfert 2 and NLRGs

Galaxy	$\log T$ (K)	$\log n_e$ (cm^{-3})	$E(B-V)$
Mrk 3	4.1	3.5	0.50
Mrk 34	4.1	3.2	0.30
Mrk 78	4.0	3.2	0.72
Mrk 198	4.1	2.6	0.24
Mrk 348	4.2	3.3	0.41
3C 33	4.1	2.9	0.38
3C 98	4.3	3.6	0.68
3C 327	4.3	3.2	0.43
3C 433	4.2	2.4	0.58

13.5 Photoionization

- Photoionization is the main ionization mechanism.
  - The temperature in the ionized gas in Cyg A and other NLRGs and Seyfert 2 galaxies $\sim 1-2\times10^4$ K.
  - In some Seyfert 2s and NLRGs, [O III] ($\lambda4959+\lambda5007$)/$\lambda4363$ is smaller, indicating higher temperature (up to $T\approx5\times10^4$ K in some objects) and $n_e<10^4\,\mathrm{cm}^{-3}$, or $T\approx1-2\times10^4$ K and higher densities (up to $n_e\approx10^7\,\mathrm{cm}^{-3}$).
  - These results strongly indicate that the main source of energy input is by photoionization.
  - **Under photoionization conditions, there is no direct relationship between gas temperature and degree of ionization.**
  - The radiative cooling by collisionally excited line radiation increases rapidly with increasing temperature, and this tends keep temperature $T\approx1-2\times10^4$ K over a wide range of input ionization radiation spectra.
- Shock-wave heating?
  - **Under pure shock-wave (or collisional) heating, there is a direct relationship between temperature and degree of ionization**, and the [O III] lines would be radiated mostly at $T>5\times10^4$ K.
  - In actual cases of shock-wave heating, pre-heating ahead of the shock front due to photoionization by radiation from the very hot gas close to the front. In this case, the [O III] emitting zone in shock gas always has $T>3\times10^4$ K.
- The observations indicates that photoionization is operative in all (or most) AGNs, since the [O III] line ratios cannot be caused by collisional ionization.

- Ionization source with "Hard" spectrum
  - This simple analysis strongly implies that photoionization is the main energy-input mechanism.
  - However, it is clear that the main source of the radiation cannot be hot stars, as in H II regions and PNe. Radiation from such stars will not produce the wide range of ionization observed in NLRG and Seyfert 2 AGNs (emission lines of low stages [O I] and [S II[, and high stages [Ne V] and [Fe VII])
  - What is required is a source with a much "harder" spectrum, that extends even further into the UV than the spectra of central stars of PNe, some of which have effective temperature up to $T = 2 \times 10^5$ K.
  - High-energy photons ($h\nu > 100$ eV) produce **high ionization (up to Ne^{+4}, Fe^{+6}, and even Fe^{+9}) near the source**, and **a long, partially-ionized "transition zone"** in which H^0 and H^+, O^0, and S^+ all coexist, and strong [O I] and [S II] lines can be collisionally excited.
  - The width of this transition zone is roughly one mean free path of an ionizing photon,

$$l = \frac{1}{n(\mathrm{H}^0)\sigma_\nu^{\mathrm{pi}}(\mathrm{H}^0)}$$

Since both $n(\mathrm{H}^0)$ and the mean frequency of the remaining photons vary rapidly with distance, the mean free path also varies rapidly.

The higher the energy of the photons present, the longer their mean free path is, and the larger the transition zone is.

- Spectral Energy Distributions (SEDs) of AGNs
  - A featureless continuum, extending across a broad range wavelengths, is observed in AGNs. The form of the SED in the optical-UV region approximately fits a power law:

    $$L_\nu = C\nu^{-\alpha}, \text{ typically with } \alpha \approx 1 - 2.$$

  - In Cyg A, the "observed" continuum has $\alpha = 3.8$. But, if it is corrected for the same amount of extinction as derived from the Balmer decrement, this becomes $\alpha = 1.6$.

    If this spectrum (with $\alpha = 1.2$, and normal abundance) extended to high energies, its can explain the observed Cyg A line spectrum.

  - A power law can both fit the observed continuum and produce reasonably strong [O I], [S II], [Ne V], and [Fe VII], emission lines.

  - The real physical situation in an AGN is no doubt much more complicated than can be represented in any simplified model.

    All nebulae have often large-scale gradients, and always with small-scale knots, filaments, and density condensations.

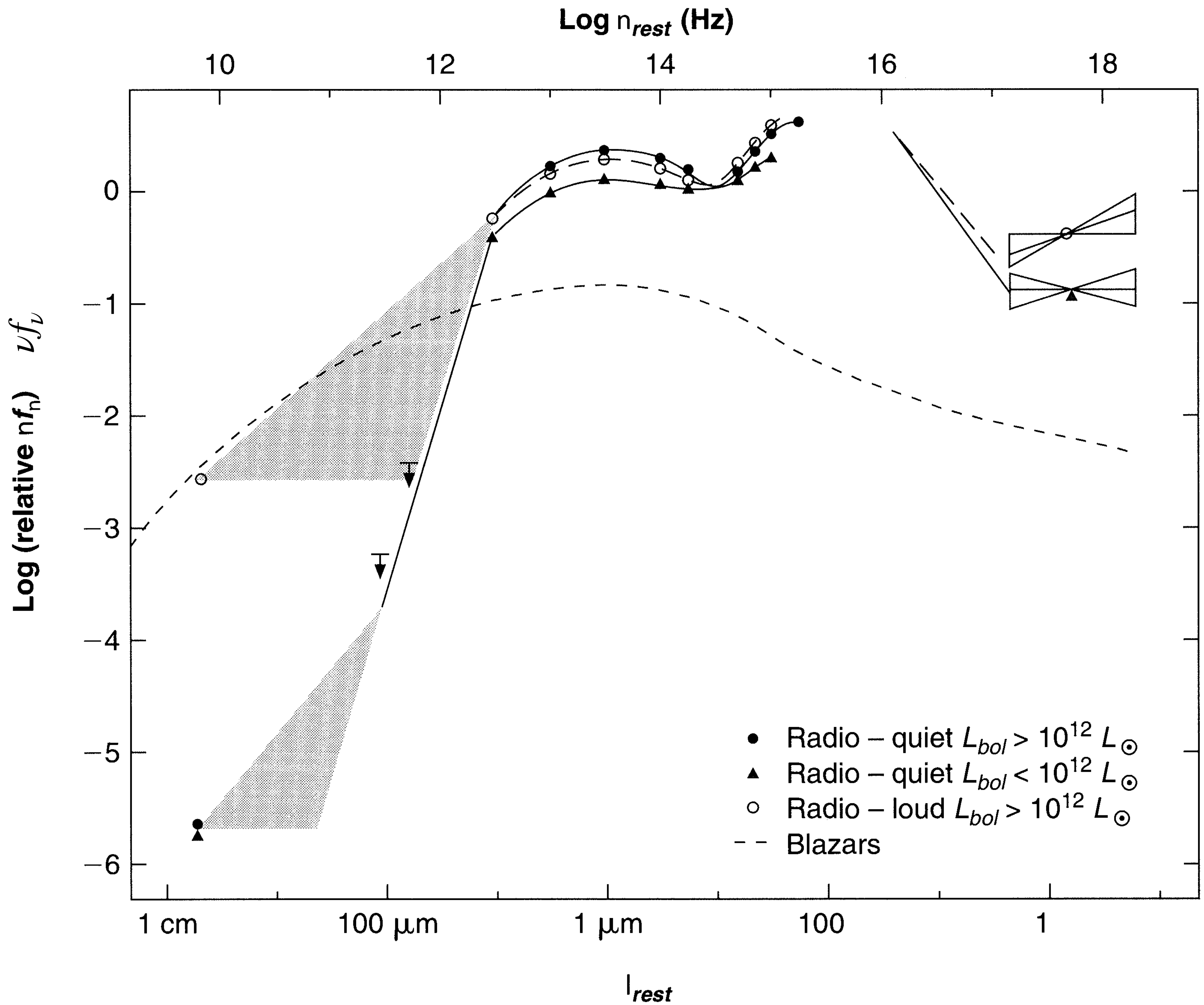

[Figure 13.7]
Spectral energy distributions for several sets of active nuclei. A horizontal line on this plot corresponds to $L_\nu \propto \nu^{-1}$, and roughly approximates the energy distribution from IR wavelengths to X-ray energies.

- Comparison with the spectrum of the Crab Nebula
  - The Crab Nebula is known to be photoionized by an UV synchrotron radiation continuum with $\alpha = 1.2$.
  - Therefore, a direct comparison of the two spectra (Cyg A and Crab nebula) is independent of any model.
  - The overall agreement is quite good, not in detailed numerical values but in which lines are strongest, which are weakest, etc.
  - Discrepancies: the He I and He II lines are stronger in the Crab Nebula, but this is because of the large He abundance in the Crab Nebula.

Table 13.2
Observed and calculated relative line fluxes in Cyg A

dust-corrected

Ion	λ (Å)	Relative Fluxes Measured	Corrected	Crab Nebula	Photoionization Model
[Ne V]	3346	0.14	0.38	—	0.12
[Ne V]	3426	0.36	0.95	0.46	0.34
[O II]	3727	2.44	5.00	10.3	0.24
[Ne III]	3869	0.66	1.23	1.56	0.53
[Ne III]	3967	0.22	0.40	0.47	0.16
[S II]	4072	0.14	0.23	0.31	
Hδ	4101	0.17	0.28	0.31	0.26
Hγ	4340	0.32	0.46	0.61	0.47
[O III]	4363	0.16	0.21	0.19	0.19
He I	4471	≤0.07	≤0.09	0.28	0.02
He II	4686	0.25	0.28	0.53	0.18
Hβ	1.00	1.00	1.00	1.00	1.00
[O III]	4959	4.08	3.88	2.81	6.3
[O III]	5007	13.11	12.30	8.43	18.1
[N I]	5199	0.40	0.32	—	—
[Fe XIV]	5303	≤0.10	≤0.08	—	0.01
[Fe VII]	5721	≤0.10	≤0.06	—	0.03
[N II]	5755	0.14	0.09	0.11	—
He I	5876	0.13	0.08	0.79	0.06
[Fe VII]	6087	≤0.07	≤0.04	—	0.04
[O I]	6300	2.10	1.10	1.20	1.24
[O I]	6364	0.69	0.35	0.33	0.41
[Fe X]	6375	0.10	0.05	—	0.07
[N II]	6548	3.94	1.90	1.56	0.29
Hα	6563	6.61	3.08	3.28	2.85
[N II]	6583	13.07	6.15	4.69	0.86
[S II]	6716	3.65	1.66	5.00	
[S II]	6731	3.29	1.51	—	
[Ar III]	7136	0.64	0.25	0.38	—
[O II]	7325	0.35	0.13	0.50	—
[Ar III]	7751	0.13	0.043	—	—

- Another check on the photoionization idea
  - The total number of ionizing photons must be large enough to balance the total number of recombinations in the ionized gas. $\Rightarrow$ related directly to the total number Hβ photons. The luminosity of Hβ is

$$L_{\mathrm{H}\beta} = h\nu_{\mathrm{H}\beta}\frac{\alpha^{\mathrm{eff}}_{\mathrm{H}\beta}(\mathrm{H}^0,T)}{\alpha_{\mathrm{B}}(\mathrm{H}^0,T)}\frac{\Omega}{4\pi}\int_{\nu_0}^{\infty}\frac{L_\nu}{h\nu}d\nu \;\Rightarrow\; L_{\mathrm{H}\beta} = h\nu_{\mathrm{H}\beta}\frac{\alpha^{\mathrm{eff}}_{\mathrm{H}\beta}}{\alpha_{\mathrm{B}}}\frac{\Omega}{4\pi}\frac{C}{h\alpha}\nu_0^{-\alpha} \quad \left(L_\nu = C\nu^{-\alpha}\right)$$

  where $\Omega/4\pi$ is the nebular covering factor and $\alpha^{\mathrm{eff}}_{\mathrm{H}\beta}(\mathrm{H}^0,T)/\alpha_{\mathrm{B}}(\mathrm{H}^0,T) \approx 1/8.5$ is the number of Hβ photons produced per hydrogen recombination.

  - It is convenient to express $L_{\mathrm{H}\beta}$ in terms of its equivalent width w.r.t. the neighboring continuum.

$$L_{\mathrm{H}\beta} = L_\lambda(\lambda 4861)W_\lambda(\mathrm{H}\beta) = L_\nu(\lambda 4861)\frac{d\nu}{d\lambda}W_\lambda(\mathrm{H}\beta) \;\Rightarrow\; W_\lambda(\mathrm{H}\beta) = \frac{L_{\mathrm{H}\beta}}{L_\nu(\lambda 4861)(d\nu/d\lambda)}$$

$$\boxed{W_\lambda(\mathrm{H}\beta) = \frac{\lambda_{\mathrm{H}\beta}}{\alpha}\frac{\alpha^{\mathrm{eff}}_{\mathrm{H}\beta}(\mathrm{H}^0,T)}{\alpha_{\mathrm{B}}(\mathrm{H}^0,T)}\frac{\Omega}{4\pi}\left(\frac{\nu_0}{\nu_{\mathrm{H}\beta}}\right)^{-\alpha} \approx \frac{568}{\alpha}\frac{\Omega}{4\pi}(5.33)^{-\alpha} \;\; [\text{Å}] \;\text{ at }\; T = 10^4\ \mathrm{K}}$$

  - This equation is satisfied if all the incident hydrogen ionizing photons are absorbed in ionization processes in the gas.

    If some escape (through density bounded regions) in some directions, so that $\Omega/4\pi < 1$ or are absorbed by dust, the right-hand side is an upper limit of W_λ.

- The observed $W_\lambda(\mathrm{H}\beta)$ measured with a slit $2.7'' \times 4''$ is ~ 39Å.
- The observed continuum is diluted by the integrated stellar absorption-line spectrum of the host galaxy. This is always a problem with NLRGs and Seyfert 2 galaxies, as well as for many Seyfert 1s.

  From an analysis of its spectrum, the fraction of featureless continuum is $f_{\mathrm{FC}} = 0.6$ and the galactic stellar continuum is $f_{\mathrm{G}} = 0.4$.
- Therefore, the corrected equivalent with of H, measured in terms of the featureless continuum, is $W_\lambda(\mathrm{H}\beta) = 39/0.6 = 65$Å.

  This is consistent with $\alpha = 1.2$.

• There is little doubt that a hard-photon spectrum, extending to X-ray energies, is the primary energy-input mechanism to the observed gas in Seyfert 2 and NLRGs.

- The narrow emission-line spectra of BLRGs and Seyfert 1 galaxies are quite similar to the spectra of NLRGs and Seyfert 2s.
  - The difference is that the ionization goes up to a higher level (strong [Fe VII] and [Fe X]) in a large proportions of the NLRs (narrow line regions) in Seyfert 1 galaxies than in Seyfert 2s.

    This may indicate a difference in the shape of the ionizing spectrum at high energies, or in the fluxes of ionizing photons incident on the NLR.
  - This can be expressed in terms of the ionization parameter:

$$U = \frac{1}{4\pi r^2 c n_{\rm H}} \int_{\nu_0}^{\infty} \frac{L_\nu}{h\nu} d\nu, \text{ where } r \text{ is the distance from the source.}$$

    U represents the dimensionless ratio of the ionizing photon density to the electron density.

The mass and size of the NLRs:

- The luminosity emitted in a recombination line, most conveniently Hβ, can be written

$$L({\rm H}\beta) = n_e n_p \alpha^{\rm eff}_{{\rm H}\beta} h\nu_{{\rm H}\beta} V\varepsilon \text{ [erg s}^{-1}\text{]},$$

  where V = total volume of the NLR and ε = filling factor.
- The mass of ionized gas is $M = (n_p m_p + n_{\rm He} m_{\rm He})V\varepsilon$.
- Assume that (1) solar abundances, (2) He is an equal mix of He$^+$ and He^{++}.

  Then, $n({\rm He}) = 0.1 n_p$ and $n_e = [n_p + 1.5 n({\rm He})] = 1.15 n_p$

- The volume of a spherical NLR is $V = \dfrac{4\pi}{3} R^3$ [cm^3].
- The most luminous Seyfert 2s or NLRs of Seyfert 1 have $L(\mathrm{H}\beta) \approx 2 \times 10^8 L_\odot$
  - This gives $M_{\rm ion} \approx 7 \times 10^5 (10^4/n_e) M_\odot$ and $R \approx 20\varepsilon^{-1/3}(10^4/n_e)^{2/3}$ pc.
  - For $n_e = 10^4\,\mathrm{cm}^{-3}$, $M_{\rm ion} \approx 10^6\,M_\odot$, and for an assumed filling factor $\varepsilon \approx 10^{-2}$, $R \approx 90\,$pc.

  The presence of low-ionization lines such as [O I] $\lambda 6300$ shows that an $\mathrm{H}^0 - \mathrm{H}^+$ ionization front must be present, so this is a lower limit to the total mass present.
- The nearest Seyfert 2 NLRs have been resolved on direct narrow-band images, and have diameters of order $10^2 - 10^3$ pc. This agrees with the above estimation.

13.6 Broad-Line Region

- Characteristic spectral feature of Seyfert 1 and 1.5 galaxies, and BLRGs
  - Broad permitted H I emission lines
  - Weaker broad He I lines, particularly λ5876, and usually broad He II λ4686
  - Most of them have broad Fe II $\lambda\lambda$4570, 5250 features, with a considerable range in strength from one galaxy to another.
  - UV Fe II features: These optical Fe II features are considerably fainter in BLRGs, but weakly present.
    - Even if they are too weak to see, the much stronger Fe II features in the UV are always detected, if the UV is observed.
    - The same broad H I, He I, He II, and Fe II emission lines are also seen in quasars and QSOs, including the blue bump ($\lambda\lambda$2000 – 4000 region).
    - The "blue bump" or "little blue bump" (in the $\lambda\lambda$2000 – 4000 region) is composed of many unresolved Fe II lines, plus the H I Balmer continuum and higher-order Balmer lines.
- **Density**
  - All the broad emission lines observed in AGNs are permitted or intercombination lines.

    None of the forbidden lines have similar broad profiles.
  - The broad lines arise in a region in which the density is so high that all the levels of abundant ions which might otherwise give rise to forbidden-line emission are collisionally deexcited.
  - The broad lines are emitted in a region in which the electron density is considerably higher than the critical densities n_c of all these levels, so that lines which would have are weakened.

- **[Lower limit of the electron density]**
  - Therefore, a quantitative estimate is rather difficult to make. Any possible broad component of [O III] λ5007/Hβ is perhaps at most 1% of that observed in narrow-line objects.
  - Since the critical density $n_c(\text{OIII}\,^1D_2) \approx 10^6\,\text{cm}^{-3}$, the electron density in a BLR is roughly $n_e > 10^8\,\text{cm}^{-3}$.
- **[Upper limit of the electron density]**
  - There is no broad lines in the optical spectral region which can be used to set an upper limit.
  - But, in the UV, C III] λ1909 has been observed with a broad profile, similar to the H I profile in several Seyfert 1 galaxies and BLRGs.
  - Broad C III] λ1909 emission is also observed in spectra of many QSOs and quasars.
  - Thus, the electron density in the C^{+3} zone must be $n_e \leq n_c(\text{CIII}\,^3P_1) \approx 10^{10}\,\text{cm}^{-3}$.
  - An intermediate value, $n_e \approx 10^9\,\text{cm}^{-3}$ may be adopted as roughly representative of the mean electron density in observed BLRs.
  - There may be regions of even higher density within the BLR. In this case, their contribution to C III] must be small.

- **Temperature & Total Mass**
  - There is practically no direct information on the temperature in the BLR. There is no straightforward diagnostics to determine T from the H I, He I, and He II lines.
  - The observed Fe II emission indicates that $T < 35{,}000\,\mathrm{K}$.
    - At higher temperature, Fe is nearly completely collisionally ionized to Fe^{++}, even if there were not ionizing photons present.
    - $T \approx 10^4$ K might be an good approximation.
  - The observed Balmer decrements in BLRs show that other processes in addition to recombination must contribution to the emission in the H I lines.
    - However, the simple recombination calculation probably gives a rough idea of the amount of ionized gas in the BLR.
    - The most luminous AGNs of Seyfert 1 and BLRGs have $L(\mathrm{H}\beta) \approx 10^9 L_\odot$, which gives $M_{\mathrm{ion}} \approx 36 M_\odot (10^9/n_e)$ and $R = 0.015 \varepsilon^{-1/3} (10^9/n_e)^{2/3}$ pc.
    - This is only the mass in ionized gas. The presence of low-ionization lines (O I λ1304) suggests a partially ionized region. Thus, there must also be uncounted reservoirs of neutral gas in the BLR.
- **Size**
  - The dimensions of BLRs are small. For $n_e \approx 10^9\,\mathrm{cm}^{-3}$, $M_{\mathrm{ion}} > 40 M_\odot$, and $\varepsilon \approx 10^{-3}$, the radius is $R \approx 0.07$ pc ≈ 0.2 light yr.
  - This is too small to be resolved even for the nearest BLR.

- However, the broad emission line profiles and fluxes have been observed to vary on time scales as short as a week or two.

  The time lag between a continuum variation and that of the emission lines has been measured, as shown in Table 13.6.

- A detailed physical model of the distribution of emitters is needed to convert the time lags into physical distances.
  - Gas that lies along our line of sight to the continuum source will have no lag.
  - However, gas on the opposite side of the central ionizing source will have a lag that is twice the light-travel time between the central engine and gas.

- The range of lags indicates that the BLR is highly stratified.
  - Higher ionization species have shorter lags, and so originate at smaller distances from the central engine than low-ionization species.

- By contrast, variations in the NLR spectra occur on very long time scales.

Table 13.6

Emission lines and continua fluxes and lags in NGC 5548

Ion	Wavelength (Å)	Flux (10^{-14} erg s^{-1} cm^{-2})	Lag (days)
Lα	1216	694	10
N V	1240	79.4	2
λF_λ	1350	5890	0
Si IV + O IV]	1400	75	—
C IV	1549	676	10
He II	1640	99	2
CIII]	1909	123	22
Mg II	2798	129	40
He II	4686	30	7
Hβ	4861	86	20
λF_λ	5100	5070	2
He I	5876	24	9
Hα	6563	316	17

- Quasars and QSOs
  - The most luminous quasars and QSOs have luminosities up to $L(\mathrm{H}\beta) \approx 5 \times 10^{10} L_\odot$, which is 50 times higher than those of BLRs.
  - Thus, they have $M_\mathrm{ion} > 2 \times 10^3 M_\odot$ and $R \approx 0.25\,\mathrm{pc} \approx 0.8$ light year.
  - Their broad lines doe not vary as rapidly as in typical Seyfert 1 AGNs.
- Nature of the energy input to the small dense BLR
  - is not obvious as it is for the NLR.
  - Most probably, it is also photoionization by the high-energy extension of the featureless continuum.
  - The most convincing evidence is provided by the correlation of the luminosities in recombination lines and in the featureless continuum (Figure 13.8).
  - In other words, all different AGNs have essentially the same Hα emission equivalent width, expressed in terms of their featureless continuum.
  - This is the result expected if all the ionization, in the NLR and the BLR, is due to photoionization by essentially the same form of input spectrum, as indicated by the following equation:

$$W_\lambda(\mathrm{H}\beta) = \frac{\lambda_{\mathrm{H}\beta}}{\alpha} \frac{\alpha^{\mathrm{eff}}_{\mathrm{H}\beta}(\mathrm{H}^0, T)}{\alpha_\mathrm{B}(\mathrm{H}^0, T)} \frac{\Omega}{4\pi} \left(\frac{\nu_0}{\nu_{\mathrm{H}\beta}} \right)^{-\alpha} \approx \frac{568}{\alpha} \frac{\Omega}{4\pi} (5.33)^{-\alpha} \quad [\mathrm{\mathring{A}}] \;\; \text{at} \;\; T = 10^4 \;\mathrm{K}$$

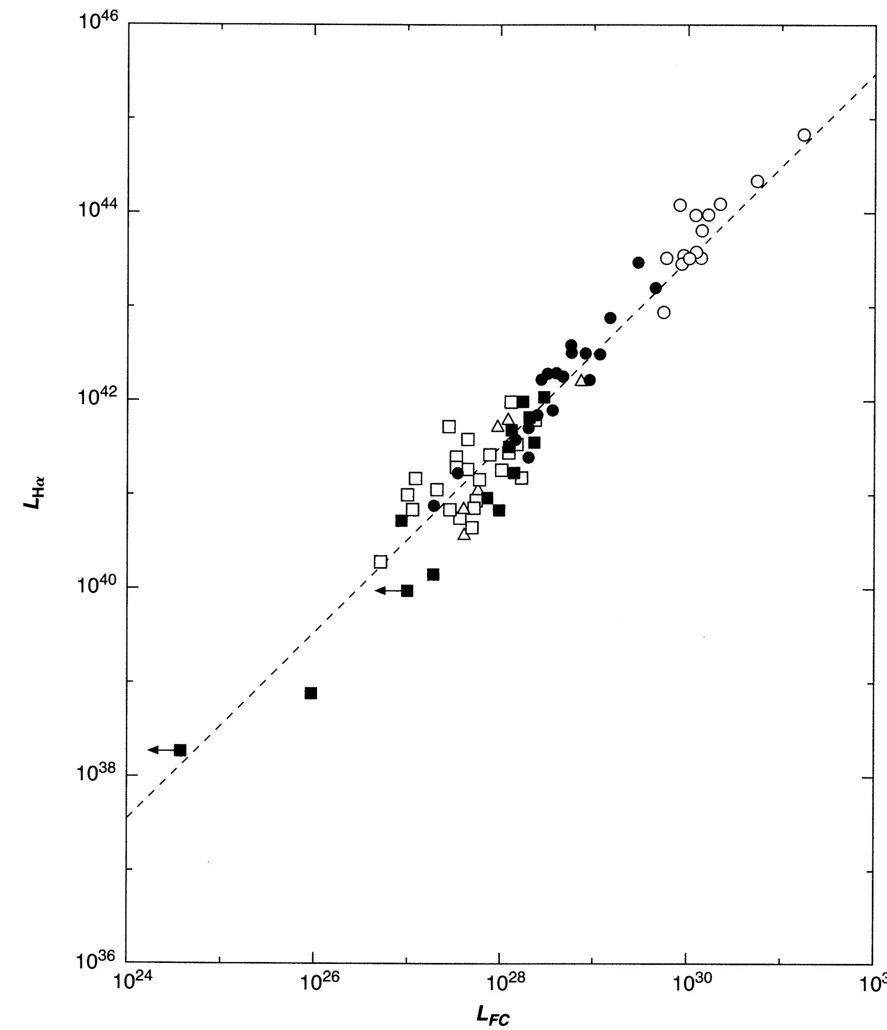

[Figure 13.8]
Luminosity in Hα (erg s^{-1}) versus luminosity in featureless continuum at λ4800 (erg s^{-1} Hz^{-1}) for QSOs (open circles), Seyfert 1s (filled circles), Seyfert 2s (open squares), NLRGs (triangles), and additional Seyfert 2 and NLRGs (filled squares). The dashed line shows the predicted relationship for a power-law photoionizing continuum with $\alpha = 1.05$

- The observations are consistent with photoionization being the energy input mechanism to the BLR as well as the NLR.
  - Typical critical densities of the optical forbidden lines is $n_c \approx 10^4\,\mathrm{cm}^{-3}$, and those of the permitted lines is $n_c \approx 10^{14}\,\mathrm{cm}^{-3}$.
  - The NLR is more distant from the continuum source, and has lower density, than the BLR.
  - Lower density gas tends to be more distant from the nucleus, and have narrower linewidths, than denser gas.

- X-ray lines such as Fe Kα
  - have critical densities of $n_c \approx 10^{20}\,\mathrm{cm}^{-3}$, even higher than the optical and UV permitted lines.
  - These X-ray lines are the inner shell fluorescent lines.
  - Figure 13.9 shows the asymmetric Fe Kα line. The separation between the line center (6.4 keV) and the extreme low-energy tail at ~ 4 keV corresponds to a velocity of $\sim 0.4c$.
  - Permitted lines in the optical and UV have critical densities $\sim 10^{14} - 10^{15}\,\mathrm{cm}^{-3}$, but do not show such broad wings.
  - Therefore, the gas emitting Fe Kα must have a density substantially higher than $10^{14}\,\mathrm{cm}^{-3}$ but less than $10^{20}\,\mathrm{cm}^{-3}$

  - The line EW is proportional to the gas column density.
  - The interpretation is that this line samples the densest gas closest to a massive black hole, and has been broadened and shifted by a combination of Doppler motions and gravitational reshifts.

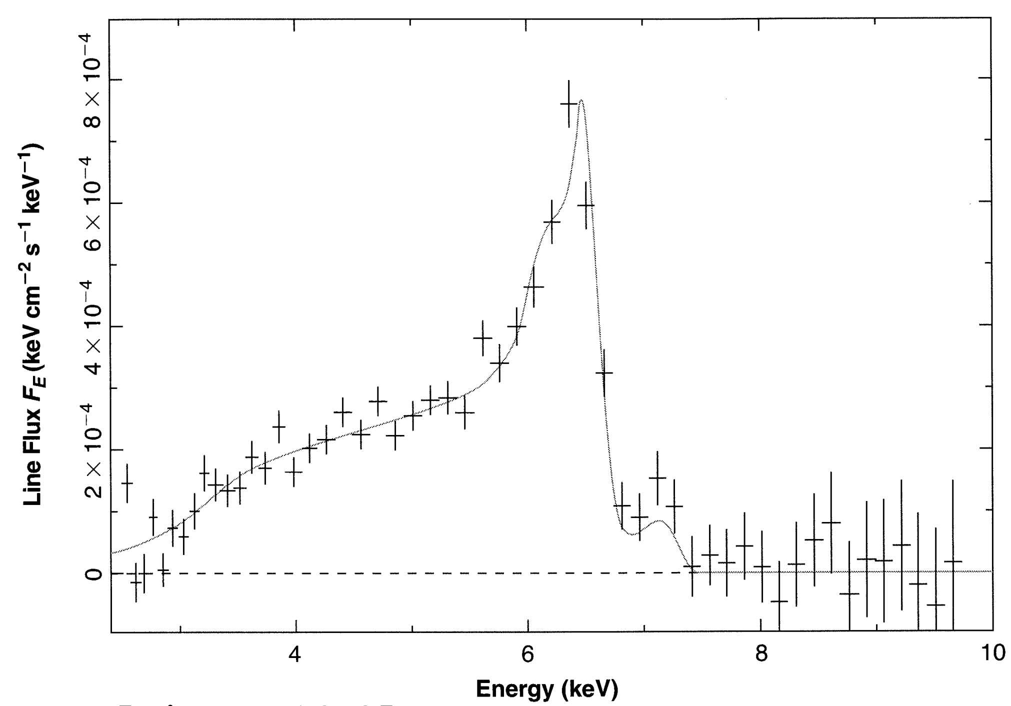

[Figure 13.9]
Fe Kα in the Seyfert 1 MCG-6-30-15.
The line center is at 6.4 keV.